

Damage to grass dikes due to wave overtopping

Le, H.T.; Verhagen, Henk Jan; Vrijling, Han

DOI

[10.1007/s11069-016-2721-2](https://doi.org/10.1007/s11069-016-2721-2)

Publication date

2016

Document Version

Accepted author manuscript

Published in

Natural Hazards

Citation (APA)

Le, H. T., Verhagen, H. J., & Vrijling, H. (2016). Damage to grass dikes due to wave overtopping. *Natural Hazards*, 86(2), 849-875. <https://doi.org/10.1007/s11069-016-2721-2>

Important note

To cite this publication, please use the final published version (if applicable).
Please check the document version above.

Copyright

Other than for strictly personal use, it is not permitted to download, forward or distribute the text or part of it, without the consent of the author(s) and/or copyright holder(s), unless the work is under an open content license such as Creative Commons.

Takedown policy

Please contact us and provide details if you believe this document breaches copyrights.
We will remove access to the work immediately and investigate your claim.

Damage to grass dikes due to wave overtopping¹

Hai Trung Le², H. J. Verhagen³, J. K. Vrijling³

Abstract:

Grass covers have been applied as an effective measure for protecting river levees and sea dikes. We conducted experiments to show how roots considerably improve the shear strength of soil on dike slopes. Roots of 1-year-old Bermuda and Carpet grass may increase the total shear strength of up to 20 kPa. Exposed to severe overtopping flow, dike slopes may possibly fail in various manners including ‘head-cut’, ‘roll-up’ and ‘collapse’. The ratio between shear strength of the grass cover and its subsoil layer would get a value of two to distinguish the first two manners and would be zero for the last one. To some extent, the findings contribute to the basis for thoughtfully investigating the strength and failure mechanism of grass-covered slopes.

Keywords: Damage, Grass cover, Root tensile strength, Sea dikes, Soil cohesion, Wave Overtopping

Contents

Damage to grass dikes due to wave overtopping.....	1
1 Introduction.....	2
2 Damage to dike slopes induced by overtopping.....	3
2.1 The wave overtopping simulator tests.....	3
2.2 Damage type ‘head-cut’.....	3
2.3 Damage type ‘roll-up’.....	4
2.4 Damage type ‘collapse’.....	5
3 Measurements of grass root properties.....	5
3.1 Species of grass on dikes.....	6
3.2 Measurement methods.....	7
3.2.1 Root diameter.....	7
3.2.2 Root distributions with depth.....	8
3.2.3 Root tensile strength.....	8
3.2.4 Cohesion of root-permeated soil.....	9
3.3 Results.....	9
3.3.1 Root diameter.....	9
3.3.2 Root distributions with depth.....	10
3.3.3 Distribution of root volume.....	10
3.3.4 Distribution of root weight.....	11
3.3.5 Distribution of root number.....	12
3.3.6 Root tensile strength.....	12
3.3.7 Cohesion of root-permeated soil.....	13
4 Parameters for determining damage to grass-covered slopes under overtopping.....	14
4.1 Root number ratio.....	14
4.2 Total root tensile strength.....	15
4.3 Root reinforcement to soil.....	16
4.4 Strength ratio and thickness ratio.....	17
5 Conclusions.....	19
References.....	19

¹ Published in Natural Hazards (Received: 13 March 2015 / Accepted: 28 November 2016/online 8-12-2017), DOI 10.1007/s11069-016-2721-2

² trunglh@wru.vn, Faculty of Marine and Coastal Engineering, Water Resources University, 175 Tay Son, Dong Da, Ha Noi, Viet Nam

³ H.J.Verhagen@tudelft.nl, Department of Hydraulic Engineering, Delft University of Technology, Stevinweg 1, 2628 CN Delft, The Netherlands

1 Introduction

Under critical conditions of weather such as storm surges, sea dikes may breach, thus resulting in serious inundations, losses of lives and properties. Many of dike failures start with erosion induced by severe overtopping flow on the inner slopes. As one of the most traditional materials, grass covers still effectively protect thousands kilometres of sea dikes all over the world. Therefore, understanding the strength of grass slopes is always critical to determine dike stability as well as the safety of land areas to be protected behind. Strength of a large number of dike slopes has been tested using the wave overtopping simulators in the Netherlands, USA and Vietnam. It was observed that a bare clay slope might fail due to a mean discharge of 1–5 l/s per m in a couple of hours (Van der Meer et al. 2009). Meanwhile, a grass-covered slope would hardly collapse under some 10 l/s per m over a similar duration (Van der Meer et al. 2009; Thornton et al. 2011; Trung et al. 2014). In the later case, dike slope has a resistance against hydraulic loads as long recognised through various experiments on slope stability, dikes and spillways (e.g. Whitehead et al. 1976; Burger 1984; Hewlett et al. 1987; Piontkowitz 2009). This strength has been proved to originate from the interaction between soil and roots (e.g. Sprangers 1999; Cazzuffi et al. 2014). In general, roots extract moisture from soil, thus resulting in desiccation and crack formation. However, the root system is likely to limit movements of soil aggregates, so binding cracks together (Coppin et al. 2007). The root system is often considered to provide an extra cohesion, hence leading to a greater shear strength of the root-permeated soil (e.g. Fan and Chen 2010; Stanczak and Oumeraci 2012; Wu 2013). Accordingly, roots improve the resistance of dike slopes against overtopping (Tuan and Oumeraci 2012; Thornton et al. 2014; Bijlard 2015).

To determine the erosion of a grass cover, theory in scouring of loosely packed and cohesive materials would be deployed (e.g. Van den Bos 2006; Hoffmans et al. 2008). In his EPM model, Van den Bos (2006) considered that the strength of a grass cover depends on the covering rate and damage often occurs at bare spots, where soil is poorly or not protected with grass. However, he did not assess the influences of grass quality. Hoffmans et al. (2008) determined critical velocity of a grass cover (or grass turf) regarding the mean bed shear stress and overtopping flow velocity. The strength of the turf presumably involves root volume, root diameter and root tensile strength. Tuan and Oumeraci (2012) estimated how roots enhance soil using a theory developed in fibre-reinforced material. Inspired by Pollen and Simon (2005), Pollen (2007), the strength mobilisation of roots was deployed to present a progressive rupture of roots during shear failure induced by overtopping.

Other works consider that both grass cover and underneath layers reserve some residual strength. Therefore, significant erosion of the grass cover may not directly lead to dike collapse but potential extending damage to subsoil layers. To describe the behaviour of dike slope under overtopping flow, Van der Meer et al. (2010) proposed several criteria such as ‘first damage’, ‘various damage locations’, ‘failure’ and ‘non-failure’. An erosional index ‘cumulative hydraulic load’ was developed to quantitatively determine these criteria regarding a critical velocity for a certain slope. The method contributes to appraise the overall condition of a slope after being loaded by a given amount of overtopping waves. Besides, experiments and theory analysis have indicated that a dike slope would be damaged at various positions in different manners. Valk (2009) emphasised the dominance of ‘head-cut’ erosion on a landward dike slope such as Afsluitdijk, the Netherlands. This mechanism was observed to take place both on the slope and at the toe of Thinh Long and Thai Tho dikes in Vietnam. In a theoretical study, Young (2005) described ‘roll-up’ as a shallow erosion of a grass turf. Similarly, a comparable mode—‘bulging’—was recorded at Boonweg dike, Friesland, the Netherlands. ‘Roll-up’ was also recognised on a 1/15-inclination slope of Yen Binh dike in Vietnam (Trung 2012). In Zeeland, a 40-cm-thick outer layer of St. Philipsland dike was severely eroded under a flow rate of 50 l/s per m, thus directly revealing a sandy core (Van der Meer et al. 2009). Aggregates torn out from the grass turf were free to fall into the sand below illustrating another manner rather than the two aforementioned.

In the context of failure study, it is essential to probably formulate the mechanisms. Obviously, a large number of simulator tests have gradually shed light on how dike slopes perform under overtopping flow. And site observations show that material composition including a grass cover and subsoil layers appears to decisively govern the manner of damage to any slope. There is little literature on defining the circumstances that facilitate certainly potential mechanism. Nevertheless, a common approach would seem to be missing to quantitatively classify damage to grass-covered slopes. Therefore, the paper intends to propose an empirical method to better describe and distinguish main types of slope damage induced by overtopping flow.

Simulator tests will be reviewed to comprehensively define recognisable types of slope damage. We investigated grass root and soil on Vietnamese dikes by applying available theories and methods in soil mechanics, plant and tree. We focused on properties such as root diameter, root distribution with depth and root tensile strength, and cohesion of rootpermeated soil. Achieved data are then analysed to study how grass roots reinforce soil. Finally, simple indicators are proposed regarding the shear strength and thickness of a grass cover and its subsoil layers to predict in which manner a certain slope may fail due to intensive overtopping flow.

2 Damage to dike slopes induced by overtopping

2.1 The wave overtopping simulator tests

To appraise the strength of dike slopes in situ, a device namely ‘wave overtopping simulator’ was first developed and deployed intensively in the Netherlands (Van der Meer et al. 2006, 2008). Similar ones were then improved and transferred to USA and Vietnam (Trung et al. 2010; Van der Meer et al. 2011; Thornton et al. 2011). The simulator is able to produce (simulate) overtopping waves, thus resulting in overtopping flow on crest and consequently on landward slope of a dike. By doing so, it is much more convenient and safer to investigate slope erosion induced by overtopping rather than during critical conditions such as storm surges.

Strength of a slope section is usually tested to suffer a certain storm of interest. And a storm is often characterised by a predefined mean overtopping discharge (e.g. 5, 10, 20, 30 l/s per m and possibly larger) and a number of overtopping waves as described in the overtopping manual EurOtop (Pullen et al. 2007). Several reports and proceedings are available describing the set-up and results of many tests in the Netherlands, USA and Vietnam (e.g. Van der Meer et al. 2009; Steendam et al. 2014; Thornton et al. 2014; Trung et al. 2014). In Vietnam, dikes were tested by the simulator at Think Long (TL), Thai Thuy (TT) and Yen Binh (YB). At every site, at least three sections of grass slope were tested. In Think Long, section TL1 was covered by only Bermuda grass. Meanwhile, Bermuda and Carpet grew together protecting sections TL2 and TL3. Sections TT1, TT2 and TT3 were protected with a mix of Bermuda and Vetiver in Thai Tho. In Yen Binh, two slope sections YB1 and YB2 were covered with Bermuda grass, while the other two YB3 and YB4 with Carpet. In general, Bermuda and Carpet grasses form a continuous mat lining over the soil surface, while Vetiver grass grows in separate clumps scattering spatially.

Under impact of overtopping flow, shallow trench and small hole might be created with a depth of some centimetres. Erosion often starts or enlarges at the transitions between slope and toe, the transitions between different materials, around objects and weak spots as observed during simulator tests in the Netherlands and Vietnam (Van der Meer et al. 2009; Steendam et al. 2014; Trung et al. 2014). Regarding various combinations of grass, soil type and layer thickness, overtopping flow may cause damage to develop further in different manners: ‘head-cut’, ‘roll-up’ and ‘collapse’.

The first two frequently take place on clayey dike slopes in Vietnamese dikes, while the last one seems to be predominant on the sandy dikes in the Netherlands. It is worth noting that the damage discussed here does not immediately lead to dike failures at functioning as sea defence. However, the slopes are destroyed to the extent that it is still feasible to repair/recover later.

2.2 Damage type ‘head-cut’

In the north of Vietnam, sea dike is usually constructed of a clayey layer and a sandy core (e.g. Trung et al. 2012). Note that only the top layer of about 20 cm thick is reinforced with grass roots, as widely reported in the literature (e.g. Sprangers 1999; Stanczak et al. 2007). On Think Long slope, some minor eroded spots were enlarged in both area and depth to expose the underneath soil. Then, the grass turf and the clayey body were likely to be eroded instantaneously. This can be explained by their similar resistance against flows. Aggregates of root-penetrated soil and lumps of clay were subtracted from the slope, thus resulting in visible holes with relatively vertical walls. These holes might extend through the clayey layer, which was about 80–100 cm thick, towards the inner core. This manner of slope destruction is defined ‘head-cut’ and sketched in Fig. 1.

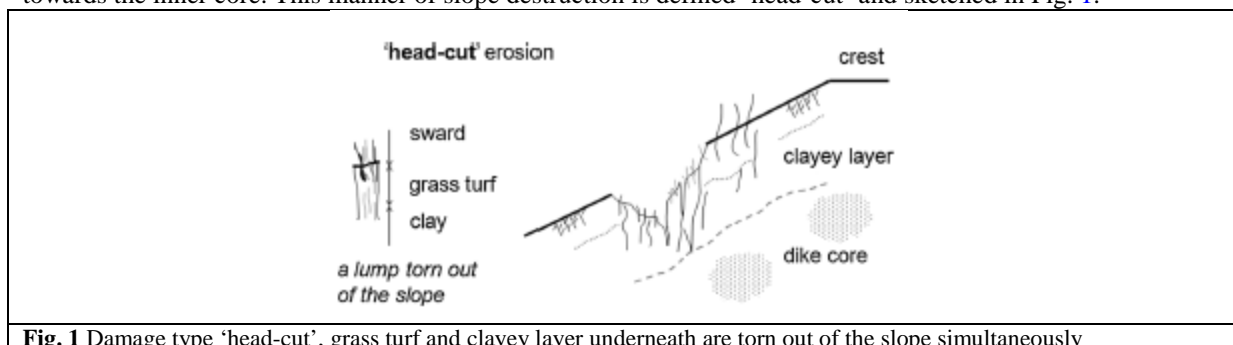


Fig. 1 Damage type ‘head-cut’, grass turf and clayey layer underneath are torn out of the slope simultaneously

Assessing tests on Afsluitdijk, Valk (2009) emphasised the dominance of ‘head-cut’ erosion on a landward dike slope, focusing on its toe. In addition, material composition would appear to play a decisive role when ‘head-cut’ took place both on the steep part and at the toe as on Think Long dike. Thai Tho dike also witnessed a similar type of erosion on the Vetiver–Bermuda grass slopes. Vetiver roots mainly develop in vertical direction, i.e. they predominantly penetrate downward rather than laterally. For this reason, soil aggregates bonded with roots are torn out of the surroundings mostly in vertical direction when exposed to overtopping flow.

Damage to grass dikes due to wave overtopping

As we have seen, ‘head-cut’ often develops through the grass turf to a underneath clayey layer which is considerably thicker than the grass turf itself. Therefore, we hypothesise that the erosional resistance varies slightly within these two layers so that lumps including rooted soil and no-root soil are extracted instantaneously and vertically. This distinguishes ‘head-cut’ from other manners such as ‘roll-up’ and ‘collapse’, where the grass turf is far different in strength compared to the underprotected materials.

2.3 Damage type ‘roll-up’

Figure 2 illustrates how eroded areas enlarge on Yen Binh dike slopes. Discharges of 80 and 100 l/s per m for hours made the left bare strip to extend about 1 m downward. Several pieces of the turf were turned up side down at the lower edges of these two eroded areas.

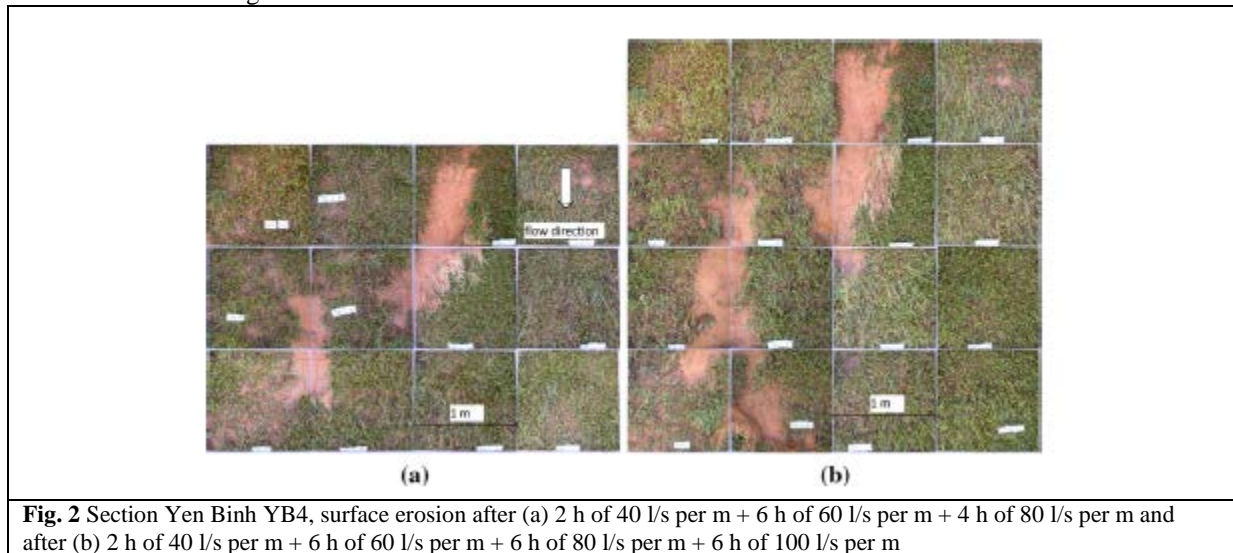


Fig. 2 Section Yen Binh YB4, surface erosion after (a) 2 h of 40 l/s per m + 6 h of 60 l/s per m + 4 h of 80 l/s per m and after (b) 2 h of 40 l/s per m + 6 h of 60 l/s per m + 6 h of 80 l/s per m + 6 h of 100 l/s per m

Figure 3 sketches this shallow surface erosion what was described as ‘roll-up’ or ‘turf set-off’ in previous works (Hewlett et al. 1987; Young 2005). The mechanism is comparable to the mode of ‘bulging’ as observed at Boonweg dike, Friesland, the Netherlands. Where several hours of 75 l/s per m flushed out a part of the grass turf revealing a hidden path constructed of brick stones (Van der Meer et al. 2008). After formation, the initial damage might probably extend towards the dike body below. Acting forces exerted by overtopping flow seem to be insufficiently energetic to destroy the layer underneath. However, flow-induced drag forces would gradually tear and lift up the grass sod, thus resulting in enlarged surface erosion.

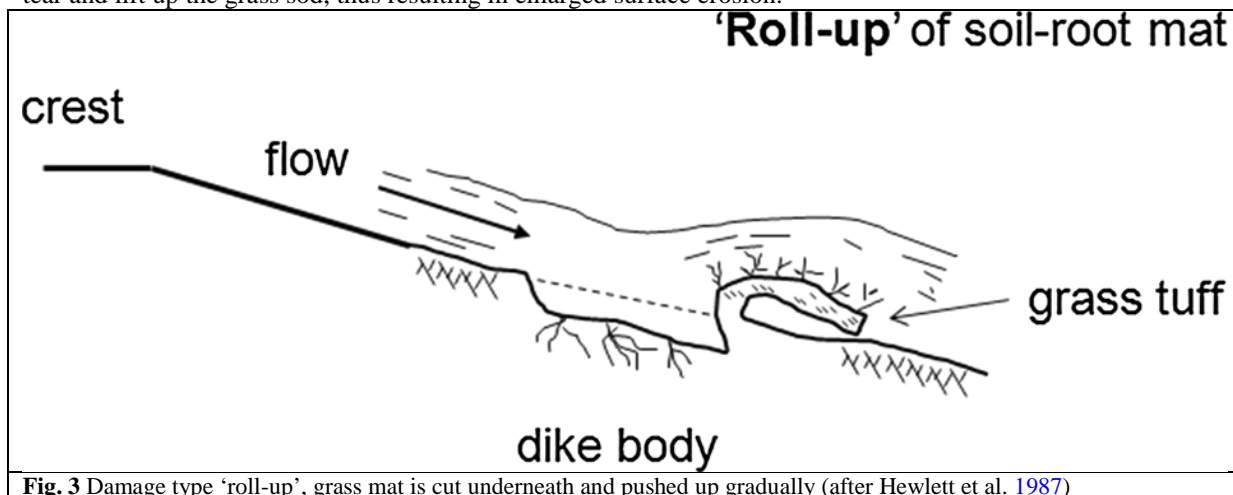


Fig. 3 Damage type ‘roll-up’, grass mat is cut underneath and pushed up gradually (after Hewlett et al. 1987)

Hoffmans (2012) proposed a turf element model to investigate the ‘bulging’ mode, in which the load is generated by the pressure fluctuations due to the flow turbulence, while the strength is a combination of soil weight, friction and root tensile. The authors pointed out that when the minimum soil normal stress falls within the grass turf and the load is sufficiently large, a ‘bulging’ mechanism might occur. Nevertheless, the Yen Binh tests suggest that critical strength should find its minimum under the grass turf and just above the hard clayey body. In other words, resistance of the underprotected soil is temporarily greater than that of the grass turf at its bottom (15–20 cm from the slope surface), thus limiting the damage from extension.

Although ‘roll-up’ could take place on slopes of both Bermuda and Carpet grass, the mechanism may show different features regarding each species. Within the first 10 cm under the soil surface, Carpet roots distribute more regularly in diameter and density, while Bermuda roots tend to get thinner and fewer as shown in Sect. 4. Besides, Bermuda grass creeps on the ground and roots wherever a node reaches the soil surface, forming a mat of stems and blades. In general, Bermuda is likely to be broken stem by stem or a group of stems which are close to each others. To contrast, due to the dense mat of roots, Carpet works as a united mat which is often lifted and rolled up at weak positions by drag forces as in Fig. 2.

2.4 Damage type ‘collapse’

In New Zealand, the Netherlands, St. Philipsland dike has an outer layer of about 40–50 cm thick including a grass turf. A flow rate of 50 l/s per m severely eroded this top layer to directly reveal a sandy core (Van der Meer et al. 2009). Because sand is noncohesive, the core was easily flushed away by water in a short period. Aggregates torn out from the grass turf were free to fall into the sand remaining below as illustrated in Fig. 4. It is the response of the slope to overtopping flows that inspires the name ‘collapse’. We hypothesised that this damage type is mainly stimulated by considerable difference between the top layer and the sandy core in their resistance to flow.

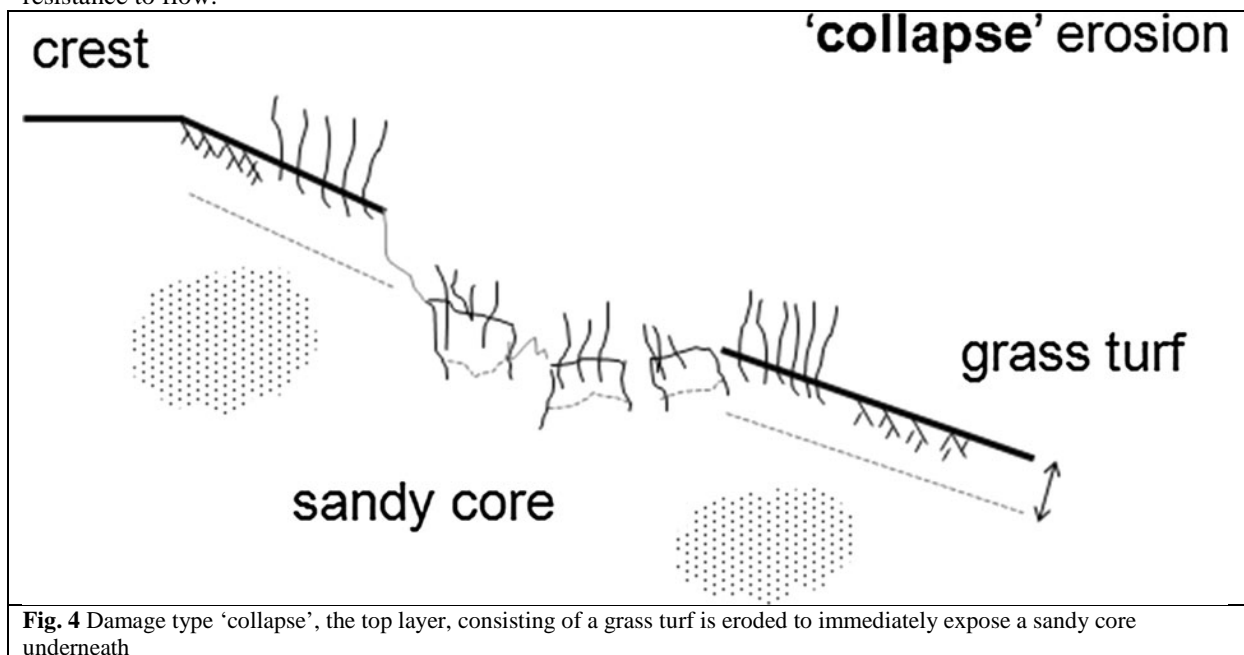


Fig. 4 Damage type ‘collapse’, the top layer, consisting of a grass turf is eroded to immediately expose a sandy core underneath

In practice, more than one single type of damage sometimes occur on one slope in a specific sequence. Simulator test on Boonweg dike, in Friesland the Netherlands, gives an example of how damage develops over three phases. After 5 h applying 75 l/s per m, two large bulges were formed and then pulled apart to expose a clayey surface underneath (first phase—‘roll-up’). ‘Head-cut’ quickly took over the thin clayey layer leading to a large hole with very steep slope (second phase). Sand was flushed out of the core leaving hollow space below the grass cover. In the third phase, lumps of clay progressively ‘collapse’ due to their self weight and overtopping flow attack. The test then stopped about 45 min after the first damage was recognised.

The presence of three layers the top soil, where most of roots are found, the subsoil of clayey and the sandy core makes three mechanisms happen on one slope like at Boonweg. Notably, much further overtopping flow would cause Think Long slopes to ‘collapse’ after the 80-cm-thick clayey layer was severely eroded to expose the sandy core. When the core material is clay instead of sand, ‘collapse’ is not likely to take place, but ‘head-cut’ would seem to be prevalent.

3 Measurements of grass root properties

Before 1991, grass covers were found as the most popular protection measure on sea dikes in Vietnam (MWRI 1991). In the last decades, the sea dike system has been improved through a considerable number of state projects. More than 80% of the landward slopes are still covered completely or partly with grass as a consequence of financial restraint rather than a design option (Trung et al. 2012).

3.1 Species of grass on dikes

Between 2009 and 2011, dikes were tested with the wave overtopping simulator in Vietnam (Trung et al. 2010, 2012, 2014). To select suitable locations, several field trips were made along the coastlines of Hai Phong, Thai Binh, Nam Dinh and Ninh Binh provinces. Figure 5 illustrates Bermuda, Carpet, Ray and Vetiver grasses, which are regularly found on sea and estuary dikes. Table 1 provides their English and Latin names.

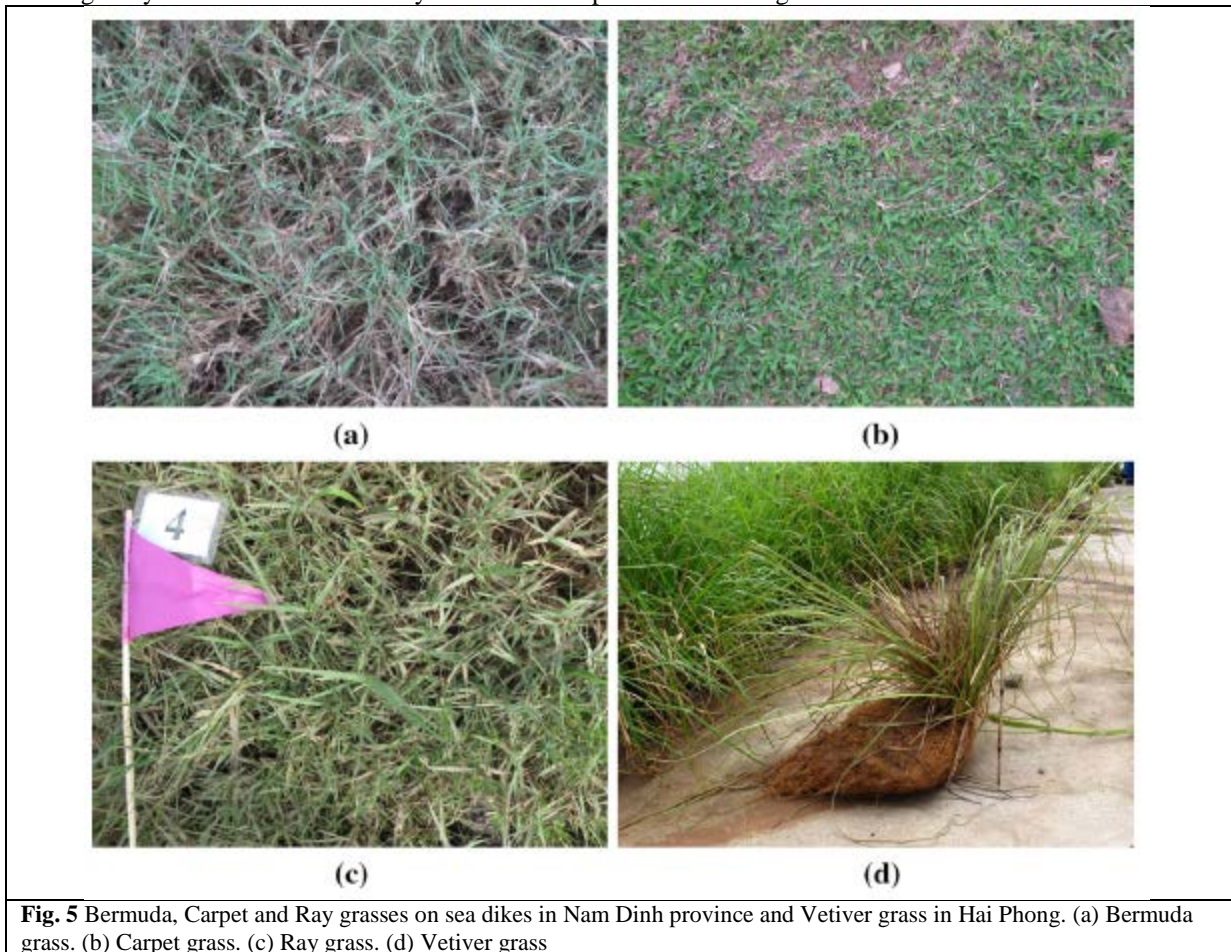


Fig. 5 Bermuda, Carpet and Ray grasses on sea dikes in Nam Dinh province and Vetiver grass in Hai Phong. (a) Bermuda grass. (b) Carpet grass. (c) Ray grass. (d) Vetiver grass

Table 1. Name of four grass species on dikes in the north of Vietnam

English	Latin	Covering type	Dike slopes
Bermuda	<i>Cynodon dactylon</i>	Mat	Thinh Long, Thai Tho, Yen Binh
Carpet	<i>Axonopus compressus</i>	Mat	Thinh Long, Thai Tho, Yen Binh
Ray	<i>Hemarthria compressa</i>	Mat	Thinh Long, Thai Tho
Vetiver	<i>Vetiveria Zizanioides</i>	Clumps	Thai Tho

Bermuda and Carpet grasses have naturally grown and manually been planted on dikes for a long time across the country. Ray grass can be found on the river-side toe in Thai Binh or on the sea-side areas in Nam Dinh. Recently, Vetiver grass (being reclassified as *Chrysopogon zizanioides*) was introduced in protecting partly the landward slope of Do Son dike in Hai Phong. Besides, Vetiver grass has also been planted in combination with other species, e.g. Carpet and Bermuda on Thai Tho dike in Thai Binh. In 2011, Bermuda and Carpet were applied to protect a 1/15-inclination dike slope which was erected for overtopping experiments in Yen Binh (Trung 2012).

It can be seen that Bermuda, Carpet and Ray grasses grow in a common pattern that evenly covers the soil surface. With a good development, they may create a continuous mat protecting the slopes. Vetiver grass, on the other hand, tends to spread across the ground in separate clumps. To protect dike slopes, Bermuda and Carpet are the most common. Vetiver with strong and long roots is durable and is commonly used in slope stabilisation (e.g. Truong et al. 2008).

Investigation of soil and grass was conducted during the simulator tests. Samples are denoted as TL after the grass names when they are taken from Thinh Long dike in Nam Dinh province, e.g. Bermuda TL and Carpet TL. Similarly, grasses from Thai Tho in Thai Binh province are added with TT and Yen Binh with YB. Bermuda,

Carpet and Ray grasses were about 4–5 years old at Thinh Long and Thai Tho. Meanwhile, grasses were about 1 year old when the investigations were carried out at Yen Binh.

3.2 Measurement methods

Root reinforcement to soil involves compound mechanisms due to various interactions between roots and soil (Cazzuffi et al. 2014). There are many factors that influence this reinforcement effect such as the size, density, Young modulus and tensile strength of roots (Greenway 1987); suction and water content, particle size, mineral composition, bulk density (Loades et al. 2010). Remarkably, how roots penetrate soil and strength properties of roots play predominant roles (Sprangers 1999; Cazzuffi et al. 2014). Root diameters may vary widely depending on species, e.g. 0.3 mm for Late Juncellus grass and 1.7 mm for Vetiver (Cheng et al. 2003). The decay of root volume is often expressed by an exponential function related to depth under the soil surface (Sprangers 1999; Stanczak and Oumeraci 2012). Meanwhile, many claim root tensile strength depends on its diameter (e.g. Tosi 2007; Comino et al. 2010). Interestingly, Zhang et al. (2014) performed biomechanical and biochemical tests to determine why root tensile strength tends to decrease with increasing root diameter. In addition, other works investigated the effect of root length and strain rate on root strength (e.g. Zhang et al. 2012). To estimate the strength of soil permeated with roots, various direct shear tests (Waldron 1977; Mickovski et al. 2010; Stanczak and Oumeraci 2012) and in situ tests (Endo and Tsuruta 1969; Fan and Chen 2010; Comino et al. 2010) were carried out. The increase in shear strength is often considered to be due to the roots via several mechanisms such as stretching, sliding, pullout and breakage (Waldron and Dakessian 1981). A large amount of measurements can be found in the literature for roots in forests (Schmidt et al. 2001), on stream banks and hill slopes (Pollen and Simon 2005; Tosi 2007; Van Beek et al. 2007) and on dike slopes (Sprangers 1999; Bijlard 2015). Using available methods in several disciplines, we carried out measurements to determine root diameter, root distribution with depth and root tensile strength, and cohesion of root-permeated soil. To measure root properties, samples including soil and roots were taken with hollow cylinders made of steel. The cylinder length could vary from 40 to 80 cm depending on grass species and soil type. For example, Vetiver roots can penetrate the soil for more than 1 m, so a length of 80 cm was applied. Roots of Bermuda, Carpet and Ray grasses concentrate within about 30 cm under the soil surface, in which case 40-cm-long cylinders were used. To take a sample, a cylinder was inserted perpendicularly into a slope to a depth of at least 30–35 cm (deeper for Vetiver). The cylinder diameters were 3 cm for determining number, 5 cm for weight and soil shear strength, and 10 cm for volume. The surrounding soil was removed away before carefully lifting the cylinder to keep the inside sample intact. After that, the soil sample was pushed out of the cylinder by a simple piece of equipment. Depending on the properties of interest, the sample could be kept as a whole or sliced into thinner parts as shown in Fig. 6a.

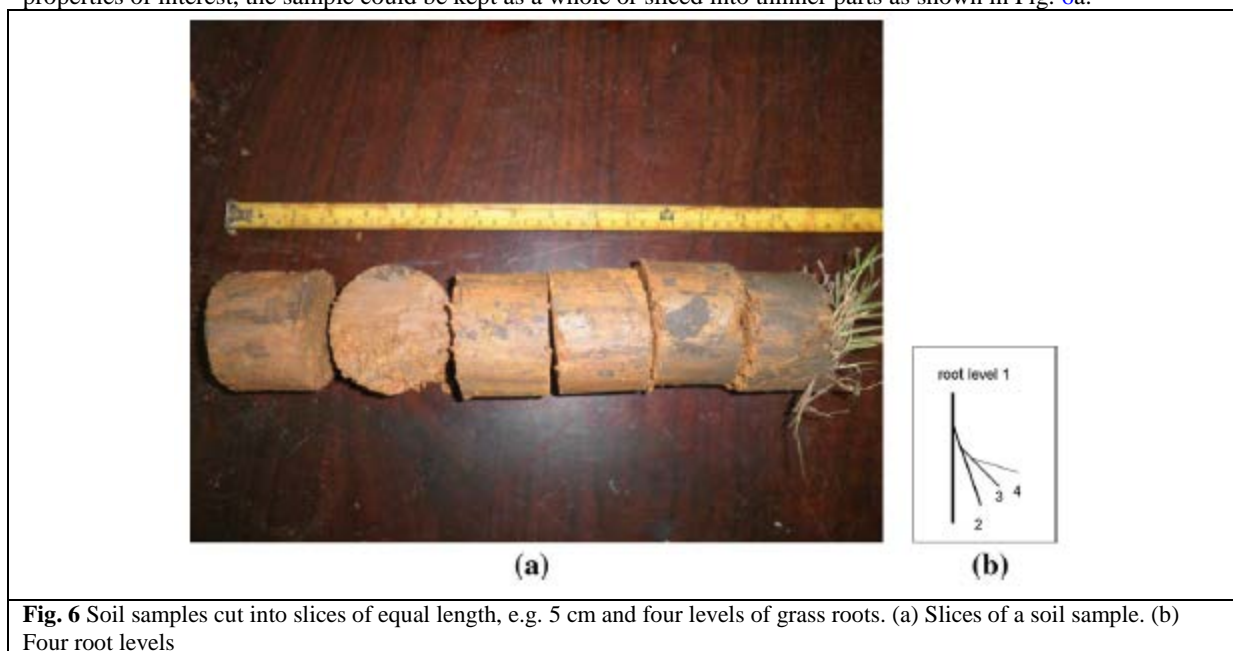


Fig. 6 Soil samples cut into slices of equal length, e.g. 5 cm and four levels of grass roots. (a) Slices of a soil sample. (b) Four root levels

3.2.1 Root diameter

Soil samples of full length were kept submerged in water for 24 h. Roots were then subtracted from soil with water sprays. After cleaning, diameter of every single root was measured using an outside micrometre (Panme) with thimble graduation of 0.01 mm. The present research classifies roots into four levels as depicted in Fig. 6b. A level-1 root is the main branch from which roots of level-2 develop. Level-3 roots directly connect to those of level-2 and so on.

3.2.2 Root distributions with depth

Root distribution can be represented by volume, weight and number with regard to depth under the soil surface. To do so, soil samples were divided into thinner slices with the same thickness as depicted in Fig. 6a. For volume and weight, soil slices of respective 10 and 5 cm thick were separately soaked in water for 24 h or longer. Roots were subtracted from soil and cleaned. The amount of roots in each slice was submerged in a vase with a known volume of water. Root volume is the difference between the water volumes (levels) in the vase before and after introducing them. This measurement follows Archimedes' principle. After cleaning, roots were dried to a stable weight. Then, dry roots in each slice were weighed using a Scientech SA 210 Model scale with a resolution of 0.0001 g.

The volume of roots contained in each slice is V_r (ml); and the total volume of roots in a sample (as a whole) is ΣV_r (ml). The percentage of root volume is defined as follow

$$\%V_r = \frac{V_r}{\Sigma V_r} 100\% \quad (1)$$

where each slice can be 10 cm thick and split from a cylinder soil sample of 30 cm long. To express the presence of roots, root volume is compared to the volume of soil where roots are embedded in. As a result, the Root Volume Ratio (RVR) is calculated as (Sprangers 1999; Stanczak and Oumeraci 2012)

$$RVR = \frac{V_r}{V_s} 100\% \quad (2)$$

in which the sample volume including soil and roots is $V_s = (\pi/4)d_s^2 h_s$ (ml or cm^3) with an associated height h_s and a diameter d_s .

The percentage of root weight is defined as

$$\%w_r = \frac{w_r}{\Sigma w_r} 100\% \quad (3)$$

where w_r is the weight of roots (g) present in each slice and Σw_r is the total weight (g) of those subtracted from the whole sample which is at least 30 cm long.

For the number, methods of sampling and investigation were inspired by a study on grass land in the Netherlands (Sprangers 1999). Soil samples were divided into slices of 3 cm thick. It is assumed that too short roots have little influence on soil so that their volume (also weight) can be neglected. Therefore, the number n_r of roots longer than 5 mm was manually counted in every slice.

The percentage of n_r is calculated as

$$\%n_r = \frac{n_r}{\Sigma n_r} 100\% \quad (4)$$

in which Σn_r is the number of roots in the entire sample, its length can be 30 cm.

3.2.3 Root tensile strength

Strength properties of plant materials such as grass roots are often represented with tensile strength and Young's modulus. Wu (2013) summarised that tensile strength of tree roots may range between 5 and 60 MPa. To determine the tensile strength of the root material, a simple tensile test may be performed on a root segment (a root thread).

Firstly, roots were carefully extracted from soil and cleaned with water sprays. To prevent roots from decay, they were wrapped in wet paper, packed into plastic bags to maintain a certain moisture and stored at a temperature of 4–5 °C. Measurements were finished in less than a week. Secondly, a single root specimen was pulled by a digital force gauge as shown in Fig. 7. Value of the breaking force F_p was documented with the corresponding diameter at the rupture point.

The tensile strength τ_r (MPa) is defined as the ratio of breaking force F_p (N) to cross-sectional area of root a_r as

$$\tau_r = \frac{F_p}{a_r} \quad (5)$$

where

$a_r = (\pi/4)d_r^2$ (m^2) and d_r (mm) is diameter at the rupture point.



Fig. 7 Root is pulled by a digital force gauge

3.2.4 Cohesion of root-permeated soil

To determine the effect of roots on soil shear strength, it is essential to assess the shear strength of root-reinforced and root-free soils. To this end, direct shear tests were performed at different depths under the slope surface. Test condition was highly saturated and undrained. Soil samples with length of at least 30 cm were cut into thinner slices, e.g. 7 or 10 cm. In fact, each of these slices was split into three pieces for testing. The obtained results were cohesion c and angle of internal friction ϕ at the middle of each slice. For example, a slice from 0 to 10 cm is characterised by c and ϕ at 5 cm under the soil surface; c and ϕ at a depth of 3.5 cm represent a slice from 0 to 7 cm. Besides, several samples were analysed more intensively to determine types and associated characteristics of soil where roots are embedded in.

3.3 Results

3.3.1 Root diameter

At Think Long and Thai Tho, up to 80% of the number of roots are of level-4 for Bermuda, Carpet and Ray grasses, and 60% for Vetiver. The average diameter of the level-4 roots varies between 0.1 and 0.2 mm. For Bermuda YB, average diameters of four levels are 0.96, 0.65, 0.37 and 0.21 mm with associated percentage of 3.35, 9.01, 15.24 and 72.41%. Roots of Carpet YB have four diameters of 1.16, 0.61, 0.4 and 0.19 mm occupying 3.82, 7.14, 12.69 and 76.36%.

Figure 8 plots root diameter d_r (mm) against corresponding percentage Per (%) of Bermuda and Carpet grasses at Yen Binh. The data suggest that these variables can be related by a function as follows:

$$Per = a_1 d_r^{b_1} \quad (6)$$

where a_1 and b_1 are coefficients derived from regression analysis. By definition, the total $S Per = \sum a_1 d_r^{b_1}$ should be approximately 100% when all roots are considered. Table 2 provides coefficients for all other grass roots at Think Long and Thai Tho.

Table 2 Coefficients of fitted curves of the relationship between root diameter and percentage, $Per = a_1 d_r^{b_1}$

Grass	a_1	b_1
Carpet TT	0.033	-4.726
Bermuda TL TT	1.421	-2.013
Ray TL TT	5.777	-1.437
Vetiver TT	10.04	-1.176
Bermuda YB	1.692	-2.364
Carpet YB	2.288	-2.093

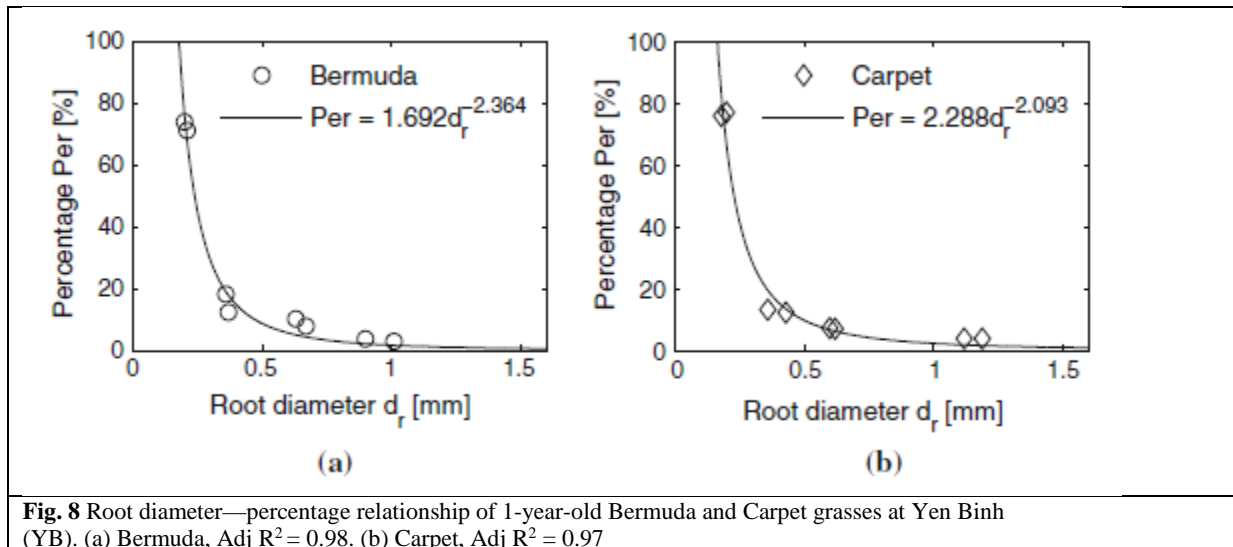


Fig. 8 Root diameter—percentage relationship of 1-year-old Bermuda and Carpet grasses at Yen Binh (YB). (a) Bermuda, Adj $R^2 = 0.98$. (b) Carpet, Adj $R^2 = 0.97$

3.3.2 Root distributions with depth

Different measurements were carried out to determine the volume, weight and number of roots. These parameters were taken at the middle of each slice, for example at depth of 5 cm for the first slice from 0 to 10 cm under the soil surface and at 15 cm for the second slice from 10 to 20 cm deep. The obtained distributions of roots with depth are presented as below.

3.3.3 Distribution of root volume

Figure 9 illustrates how root volume gradually decreases with increasing depth. The first 10 cm consists of about 50–90% of the total volume. About 10–40% concentrate in the second layer from 10 to 20 cm deep. Below 20 cm, <10% is present. In most samples, RVR is smaller than 6% within the first 10 cm under the soil surface, i.e. <6% of the total volume are roots. In the next 10 cm, RVR is usually <2%. Under 20 cm, roots occupy <1% of the total volume. The regression curve of Bermuda YB roots reads $RVR = 0.89 \times 0.75^{(d-5)}$. Note that depth d is given in centimetre.

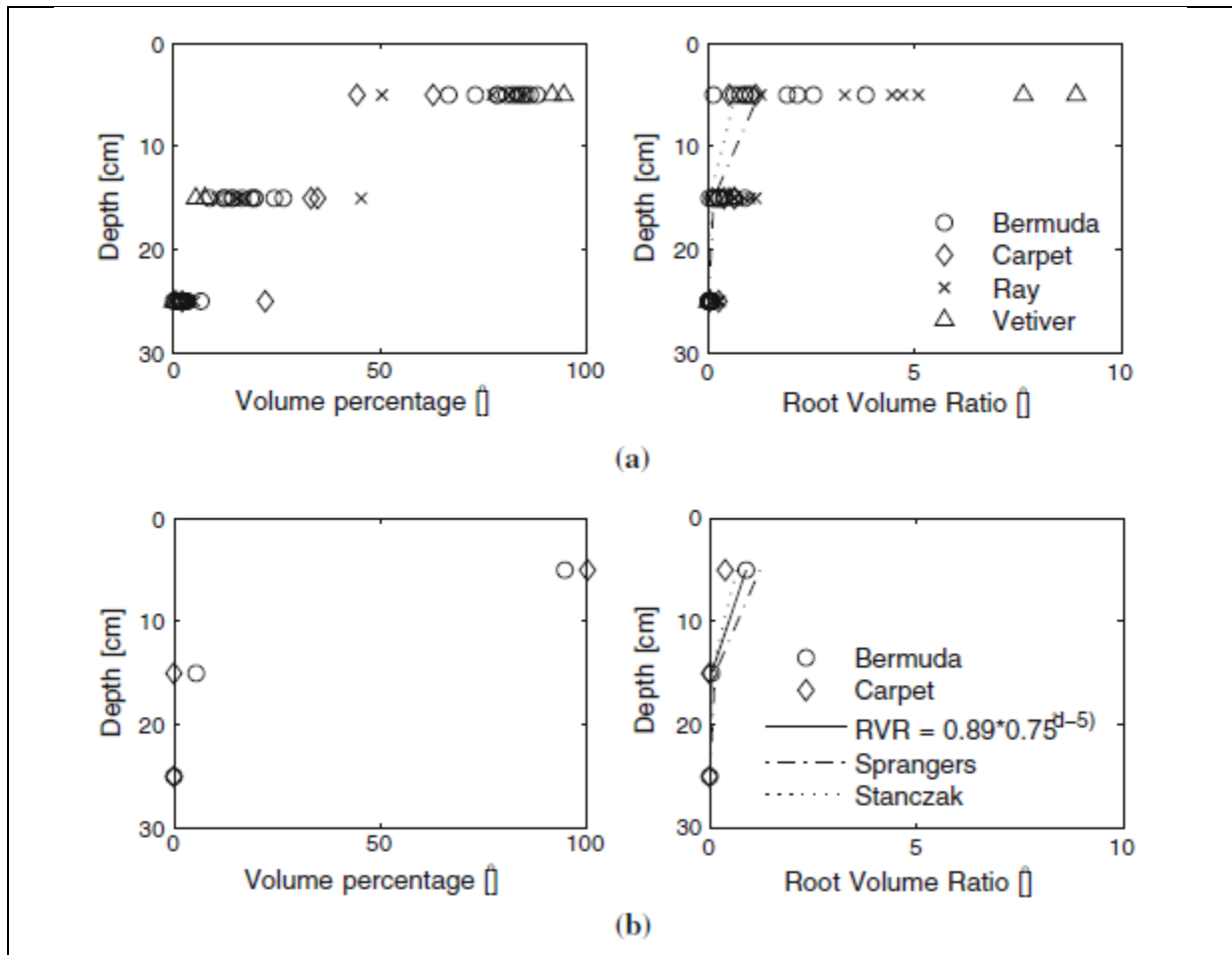


Fig. 9 Variation of root volume percentage (left) and RVR (right) with depth of grasses at Thai Tho, Think Long and Yen Binh. $RVR = 0.89 \times 0.75^{(d-5)}$ is the regression curve of Bermuda YB roots. (a) Think Long and Thai Tho dikes. (b) Yen Binh dike

3.3.4 Distribution of root weight

Figure 10 shows the decrease in weight of roots w_r with increasing depth. At Think Long and Thai Tho, grasses were about 4–5 years old giving much more weight of roots than the 1-year-old ones at Yen Binh.

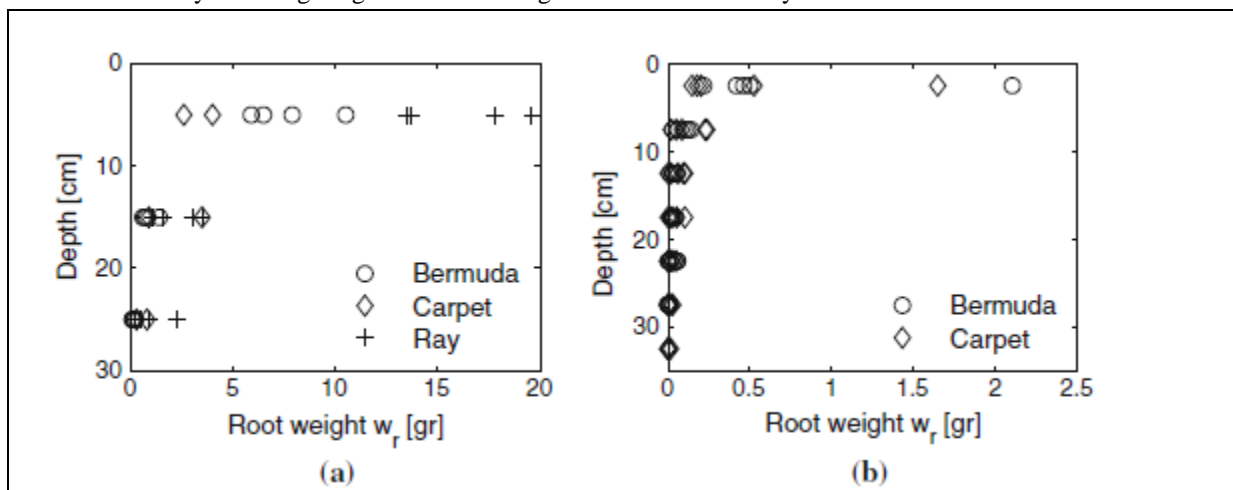


Fig. 10 Distribution of root weight w_r (g) with depth. (a) Think Long and Thai Tho, grass of 4–5 years old. (b) Yen Binh, grass of 1 year old

Besides, Figure 11 illustrates how the percentage of root weight distribute with depth. In the first 10 cm under the soil surface, 50–90% of the total weight concentrate. In the meanwhile, about 10% can be found below a depth of 20 cm. At Yen Binh, Carpet roots penetrate deeper than 30 cm from the soil surface.

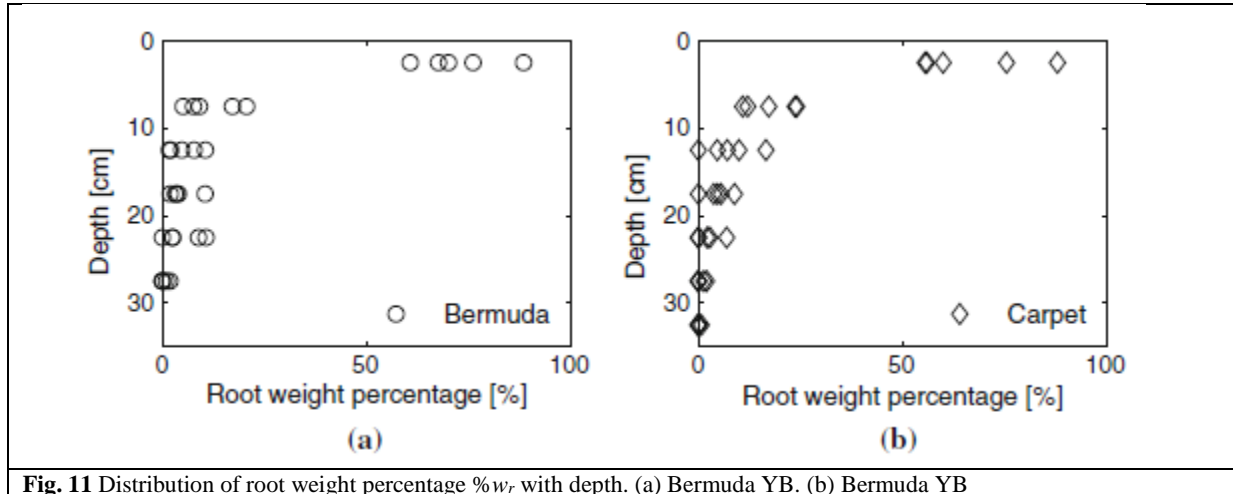


Fig. 11 Distribution of root weight percentage $%w_r$ with depth. (a) Bermuda YB. (b) Bermuda YB

3.3.5 Distribution of root number

Figure 12a shows the number of roots n_r present in 3-cm-thick slices of soil taken from Yen Binh. At the same depth, Carpet has more roots than Bermuda. There are respective 80 and 44 roots at a depth of 1.5 cm on a soil area with radius of 15 mm; and 20 and 10 ones at 20 cm on the same area. Besides, Carpet roots penetrate more deeply than Bermuda ones, up to 30 and 25 cm, respectively. Bermuda is Poor to Average condition of cover, while Carpet is Average to Good with regard to the classification given in the Dutch safety standard (VTV 2006).

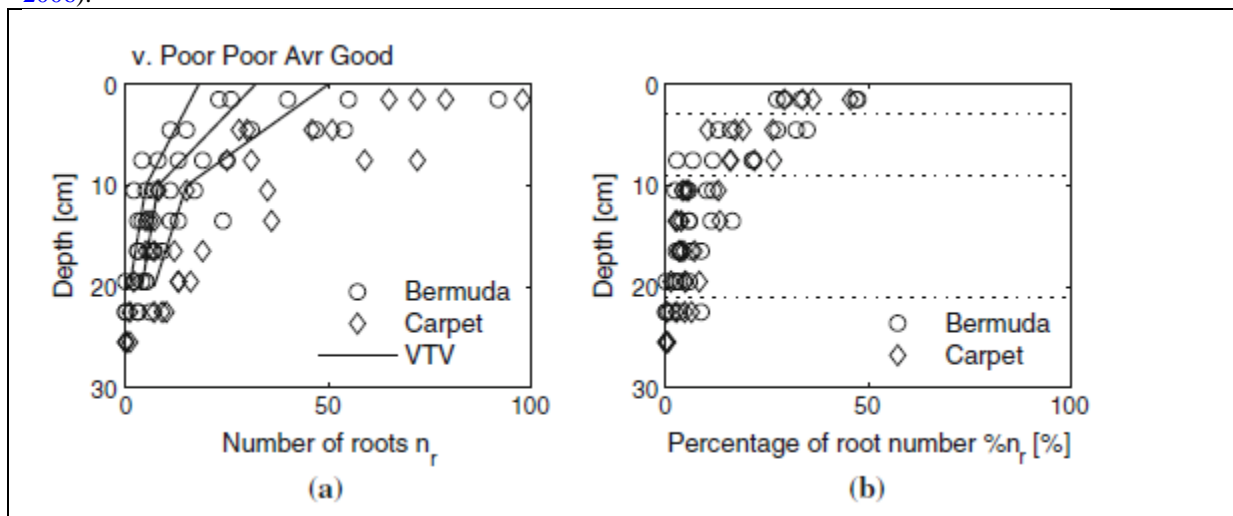


Fig. 12 Variation of root number n_r and associated percentage $%n_r$ with regard to depth of Bermuda YB and Carpet YB. Conditions of grass covers are categorised using the Dutch safety standard (VTV 2006). (a) Number of roots n_r . (b) Percentage of root number $%n_r$.

Regardless of diameter and level, about 20–60% of roots concentrate in the first 3 cm under the soil surface as shown in Fig. 12b. The first 9 cm consists of more than 50–90%. About 10–40% are present in the layer between 9 and 21 cm of depth. Below 21 cm, <10% of roots can be found. In comparison with volume and weight, the number of roots is distributed with a similar pattern with depth.

Additional measurements were conducted at Yen Binh. The 2-year-old Bermuda grass provides more than 100 roots at a depth of 1.5 cm, while only 44 roots were found 1 year earlier. Similarly, older grass has much more weight as compared in Fig. 10.

3.3.6 Root tensile strength

In general, a single root may resist a breaking force of up to 10 N. At Thai Tho, grasses were 4–5 years old except Vetiver of 6 months; while Bermuda and Carpet were one year old at Yen Binh. Most roots have τ_r of <200 MPa, e.g. see Fig. 13. And roots seem to be stronger when grass becomes more mature. The obtained

results are relatively comparable with some fibre materials such as 31 MPa for Plastic (PVC) with a diameter of 2.2 mm and 200 MPa for Copper (wire) with a diameter of 1.0 mm (Gray and Ohashi 1983).

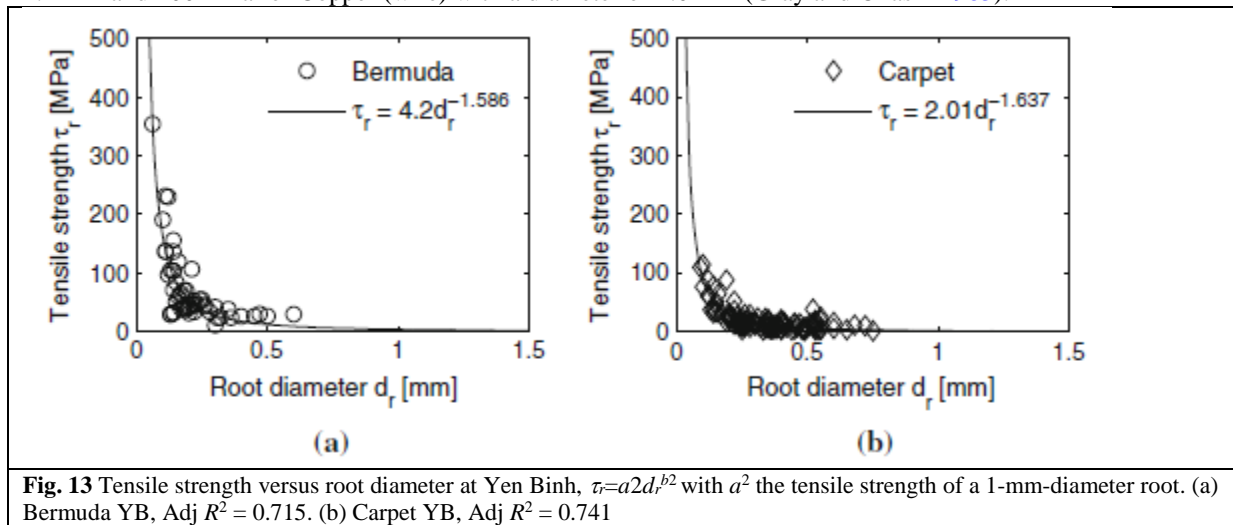


Fig. 13 Tensile strength versus root diameter at Yen Binh, $\tau_r = a_2 d_r^{b_2}$ with a_2 the tensile strength of a 1-mm-diameter root. (a) Bermuda YB, Adj $R^2 = 0.715$. (b) Carpet YB, Adj $R^2 = 0.741$

Tensile strength decreases with increasing diameter. The thicker the root, the greater the breaking force is. And the tensile strength is calculated per unit area. As a result, the thinner the root, the greater does the tensile strength become. Therefore, each data set is fitted with a power curve as proposed in earlier works (Pollen and Simon 2005; Tosi 2007; Fan and Chen 2010)

$$\tau_r = a_2 b_r^{b_2} \tag{7}$$

in which a_2 and b_2 are coefficients obtained by regression analysis. Note that a_2 represents the tensile strength of a 1-mm-diameter root. Table 3 provides the two coefficients for six data sets of grass roots at Thai Tho and Yen Binh.

Table 3 Coefficients of the fitted curves presenting the relationship between root diameter d_r (mm) and associated tensile strength $\tau_r = a_2 \times d_r^{b_2}$ (MPa), where a_2 (MPa) is the tensile strength of a 1-mm-diameter root

Grass	a_2	b_2	Adj R^2
Bermuda TT	17.070	-1.295	0.718
Carpet TT	25.410	-1.072	0.689
Ray TT	10.540	-1.431	0.757
Vetiver TT	17.220	-2.024	0.867
Bermuda YB	4.2	-1.586	0.715
Carpet YB	2.01	-1.637	0.741

3.3.7 Cohesion of root-permeated soil

At Yen Binh, direct shear tests were performed for seven cylindrical samples of soil permeated with Bermuda roots and nine samples with Carpet roots. Varying from 10 to 40 kPa, cohesion c tends to decrease with increasing depth as shown in Fig. 14. This pattern is similar to the variation in volume, weight and number of roots as described above. It would be the reduction in root amount that leads to the decrease in the total cohesion with regard to depth. The issue will be elaborated further in the next section (Table 4).

Table 4 Material specification, grass properties and damage description of 10 simulator tests in Vietnam. Grass cover quality is classified according to VTV (2006)

Sec.	Material	c_{ss} 10^3 N/m ²	Grass quality	n_r roots	$a_4 \sum \tau_r$ 10^3 N/m ²	c_{ss}/c_{turf}	d_{ss}/d_{turf}	Damage
TL1	100 cm clay, sand core	20	Good	50	11.05	1.81	4	Head-cut
TL2	80 cm clay, sand core	20	Good	50	11.05	1.81	3	
TL3	80 cm clay, sand core	20	Good	50	11.05	1.81	3	
TT1	Clay dike	20	Good	50	11.05	1.81	10	Head-cut/concrete beams
TT2	Clay dike	20	Good	50	11.05	1.81	10	
TT3	Clay dike	20	Good	50	11.05	1.81	10	
YB1	Good clay	23.07	Average	44	6.29	3.67	10	Thin 'roll-up'
YB2	Good clay	23.07	Average	44	6.29	3.67	10	
YB3	Good clay	23.07	Good	80	6.29	3.8	10	
YB4	Good clay	23.07	Good	80	6.29	3.8	10	

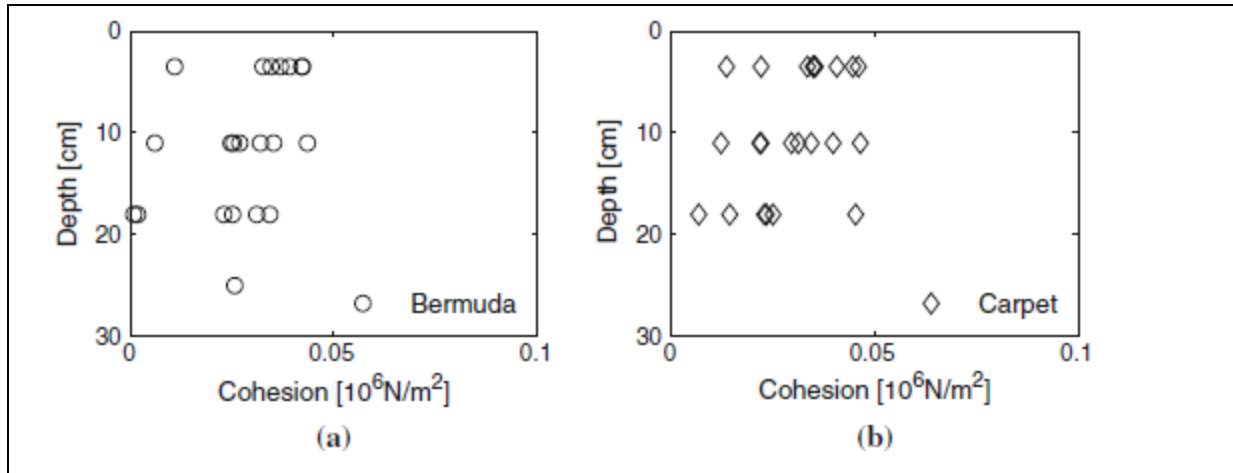


Fig. 14 Cohesion variation with depth of soil permeated with roots of Bermuda YB and Carpet YB. (a) Bermuda roots. (b) Carpet roots

Soil particle-size distributions were determined by sieve analysis and sedigraph analysis for 4/16 of the samples above (2 of Bermuda and 2 of Carpet). The soil is classified as clay with sand content of <40% regarding the current guidelines in Viet Nam (TCVN8217 2009), where sand is defined as content of grains with size smaller than 2 mm and larger than 0.05 mm. Tables 5 and 6 provide extra characteristics of these soil samples taken from Yen Binh.

Table 5 Particle-size analysis (Percentage Passing %) of selected soil samples taken from Yen Binh

Sample	Sieve size (mm)									
	>5	5.0-2.0	2.0-1.0	10.0-0.5	0.2-0.25	0.25-0.1	0.1-0.05	0.05-0.01	0.01-0.005	<0.005
B1-I-1	1.38	3.25	1.38	1.90	1.73	3.49	20.04	29.09	13.61	14.11
B2-I-1	0.95	2.07	0.82	2.10	2.27	5.23	24.69	23.95	7.59	30.34
C3-I-1	48.64	5.98	1.42	3.38	5.82	7.04	7.44	5.89	1.42	12.97
C4-I-1	43.97	11.25	3.72	3.76	2.33	2.03	25.40	2.19	0.53	4.82

All samples have length of 7 cm, from 0 to 7 cm under the soil surface. Sample name denoted by 'B' means that soil is reinforced by Bermuda roots and 'C' by Carpet roots

Table 6 Soil characteristics of selected samples taken from Yen Binh

Sample	Moisture cont. W(%)	Spec. gravity G_s (g/cm ³)	Density r (g/cm ³)	Dry density r_d (g/cm ³)	Saturation S (%)	Porosity N (%)	Void ratio e_0	Atterberg			Liquidity index LI
								Liq.lim. W_l (%)	Plast.lim W_p (%)	Plast.in. I_p (%)	
B1-I-1	39.86	2.69	1.739	1.240	91.72	53.90	1.17	48.54	32.43	16.11	0.46
B2-I-1	36.63	2,69	1.743	1.280	89.41	52.43	1.10	45.13	29.46	15.67	0.46
C3-I-1	38.79	2.69	1.762	1.270	93.33	57.79	1.12	51.23	37.76	13.47	0.08
C4-I-1	31.40	2.69	1.775	1.350	85.06	49.82	0.99	47.60	31.96	15.91	<0

4 Parameters for determining damage to grass-covered slopes under overtopping

Measurements were taken resulting in a data set on roots of four grass species on Vietnamese dikes. The obtained data show similar properties as discovered in previous works and provide distinguishing features such as thicker and stronger threads. Of course, the presence of roots exerts influence on soil. This section will further analyse the measurement results to evaluate how it affects soil. The discussion focuses on the distribution and tensile strength of roots and the cohesion of root-permeated soil. Finally, simple parameters are introduced to determine potential damage to grass-covered slopes under impact of overtopping.

4.1 Root number ratio

Data analysis has revealed that number, volume and weight of roots distribute identically with respect to depth. At a certain depth, the volume and weight are proportional to the number of roots regardless of level and size. About 60–90% of the root amount (number, volume and weight) are present within the top 10 cm under the soil surface. There are <10% under a depth of 20 cm. To express a similar distribution of root weight, Sprangers (1999) introduced an exponential function. He claimed that about 53–55% of the total roots can be found in the

first 6 cm and about 75–80% within the layer between depths of 0 and 20 cm. Besides, Reubens *et al.* (2007) characterised root architecture by using size, branching pattern and number of roots per soil area or volume. Inspired by other works, the Root Number Ratio (RNR) is proposed to show how roots distribute with depth as

$$RNR = \frac{n_r}{n_{r0}} \quad (8)$$

where n_r and n_{r0} are the numbers of roots at depths d and d_0 , respectively. And d_0 is taken at the middle of the first slice. For example, a cylindrical soil with length of 30 cm is cut into ten 3-cm-thick slices. Therefore, reference depth d_0 is 1.5 cm under the soil surface. Figure 15 shows RNR calculated for Bermuda (circle) and Carpet (diamond) roots at Yen Binh dike.

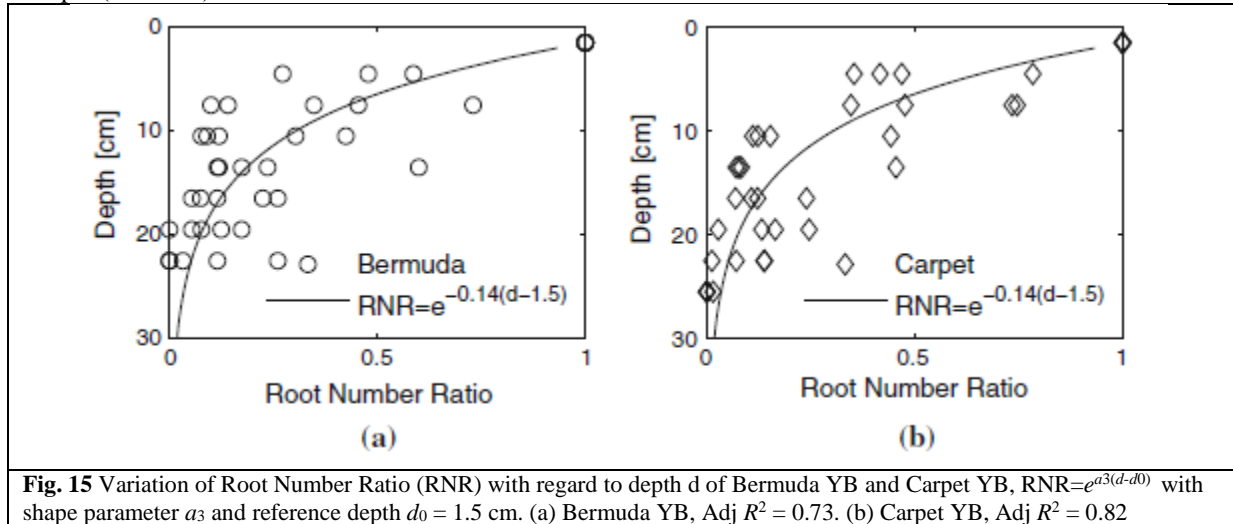


Fig. 15 Variation of Root Number Ratio (RNR) with regard to depth d of Bermuda YB and Carpet YB, $RNR=e^{a_3(d-d_0)}$ with shape parameter a_3 and reference depth $d_0 = 1.5$ cm. (a) Bermuda YB, $Adj R^2 = 0.73$. (b) Carpet YB, $Adj R^2 = 0.82$

The decrease in RNR can be expressed by an exponential function with regard to depth d as

$$RNR = e^{a_3(d-d_0)} \quad (9)$$

in which $d_0 = 1.5$ cm is the reference depth and $a_3 = -0.14$ is the shape parameter obtained by regression analysis. When n_{r0} at d_0 is known, the number of roots n_r at a certain depth d can be derived from RNR. For example, measurements have shown that $n_{r0} = 44$ and 80 of Bermuda and Carpet roots at $d_0 = 1.5$ cm on a 15-mm-radius area of soil. Using Eqs. (8) and (9) gives respective 27 and 49 roots of the two species at depth of 5 cm on the same area.

4.2 Total root tensile strength

At a given depth, there are n_r roots present on a given area of soil, e.g. a_s . Each root may break due to a certain pulling force F_p . All roots together will be able to withstand a total force, which is assumed to be greater than the pulling force of each thread. Consequently, soil including roots can be considered to possibly resist this total pulling force on the area a_s . Because soil easily fails when being pulled, so resistance of soil against pulling can be neglected. If all roots are assumed to work simultaneously, the total tensile strength that soil on the area of a_s at a depth d may have is

$$\Sigma \tau_r = \frac{\Sigma F_p}{a_s} \quad (10)$$

in which $a_s = \pi r_s^2$ (m^2) with radius r_s (mm) of the soil area, pulling force F_p (N) can be derived from τ_r and d_r as $F_p = \tau_r(\pi d_r^2/4)$. Recall the diameter–percentage relationship in Sect. 3.3, n_r is the total numbers of roots belonging to four levels. If the measured diameters of Bermuda YB are 0.96, 0.65, 0.37 and 0.21 mm, Eq. (6) derives the associated percentage of four levels as 1.89, 4.68, 18.33 and 71.68%, respectively. As a result, the total computed value is 96.58% which is very close to 100%, conserving n_r . One may write

$$\Sigma F_p = n_r \Sigma Per(d_r) F_p(d_r) \quad (11)$$

where n_r can be derived using Eq. (8) and (9), percentage Per is calculated with Eq. (6) and root tensile strength τ_r with Eq. (7). Therefore, Eq. (10) is now written as

$$\Sigma \tau_r = n_{r0} e^{a_3(d-d_0)} \Sigma (a_1 d_r^{b1}) (a_2 d_r^{b2}) \frac{\pi d_r^2}{4 a_s} \quad (12)$$

to show that the total root tensile strength exponentially decrease with depth. This means the strength of root-permeated soil against pulling decreases exponentially with increasing depth.

4.3 Root reinforcement to soil

Soil failure is normally described with the Mohr Coulomb theory by relating shear stress and effective normal stress along an frictional sliding plane as

$$\tau = c_s + (\sigma - \rho_w) \tan \phi \quad (13)$$

where τ is the soil shear strength (kPa), c_s is the effective soil cohesion (kPa), σ is the soil normal stress (kPa), ρ_w is the pore water pressure (kPa) and ϕ is the internal friction angle ($^\circ$) (Lambe and Whitman 1969). It has been seen that most roots concentrate within the top 20–30 cm under the soil surface. This layer of root-permeated soil is defined as a grass turf (Muijs 1999). In the turf, the root system provides an artificial (apparent) cohesion and causes little effect on the frictional component of strength (Gray and Megahan 1981; Waldron and Dakessian 1981; O'Loughlin and Ziemer 1982). Therefore, many authors have modified the Mohr Coulomb theory of soil failure to estimate root reinforcement to soil (Wu et al. 1979; Schmidt et al. 2001; Pollen and Simon 2005; Hoffmans et al. 2008). For example, the enhanced soil shear strength may read as

$$\tau = (c_s + c_r) + (\sigma - \rho_w) \tan \phi \quad (14)$$

with the artificial cohesion c_r induced by roots (kPa) (Waldron 1977). Root-permeated soil can now be considered as a new material with different cohesion c which is the sum of soil cohesion (without root) c_s and root apparent cohesion c_r , i.e. $c = c_r + c_s$. For comparison, the cohesion capacity was expressed to be the sum of the cohesion capacity of the soil itself and the effect of tree root system in an early study in Japan (Endo and Tsuruta 1969). To appraise the effect of roots on soil cohesion, the present study relates c_r to root tensile strength as often assumed in previous works (Wu et al. 1979; Schmidt et al. 2001; Stanczak and Oumeraci 2012). To this end, $\Sigma \tau_r$ are plotted against corresponding c at the same depth in Fig. 16a, where $\Sigma \tau_r$ is calculated with Eq. (12) using $n_{r0} = 44$ and 80 roots for respective Bermuda YB and Carpet YB at $d_0 = 1.5$ cm. Diameters of four levels 0.96, 0.65, 0.37, 0.21 mm are given to the former; and 1.16, 0.61, 0.4 and 0.19 mm to the later (see also Sect. 3.3.1). Meanwhile, Fig. 14 provides the total cohesion c measured at various depths of up to 30 cm, i.e. within the turf.

It can be seen that the decrease in c is likely to be proportional to the reduction in $\Sigma \tau_r$. If the cohesion of soil without root c_s is considered to be the same with depth, the total cohesion of root-permeated soil c is only determined by the number and tensile strength of roots. The relationship between c and $\Sigma \tau_r$ can be simply expressed by a linear function

$$c = c_s + c_r = c_s + a_4 \Sigma \tau_r \quad (15)$$

with $c_s = 23.07$ kPa and $a_4 = 0.19$ derived from regression analysis. This value of c_s are comparable to the data measured at a depth of 18 cm where the amount (i.e. influence) of roots becomes relatively minor as depicted in Fig. 14.

The measured values of c_r can be obtained by subtracting $c_s = 23.07$ kPa from the data of c given in Fig. 16a. And panel (b) indicates that root cohesion c_r may reach 15–20 kPa when 60 Carpet roots or 40 Bermuda ones are present on a 15-mm-radius area of soil. With the same amount, Bermuda roots give a higher value of c_r because of greater tensile strength. However, Carpet has more roots (higher n_r) at the same depth, for example, 49 compared with 27 at 5 cm below the ground surface (see Sect. 4.1). Consequently, the two species provide relatively comparable root cohesion when they both grow in similar soil.

Furthermore, Carpet roots penetrates more deeply so that their effect on soil is deeper (see also Figs. 10, 11, 12). Measurements have shown that the amount (weight and number) and tensile strength of roots become greater when grass is more mature. Another experimental study revealed that the root artificial cohesion increases proportionally to the fresh weight of *Betula japonica* Sieb. and *Alnus japonica* Steud. roots per m^3 of soil (Endo and Tsuruta 1969). Therefore, more mature grass is expected to improve better the shear strength of soil where roots are embedded in.

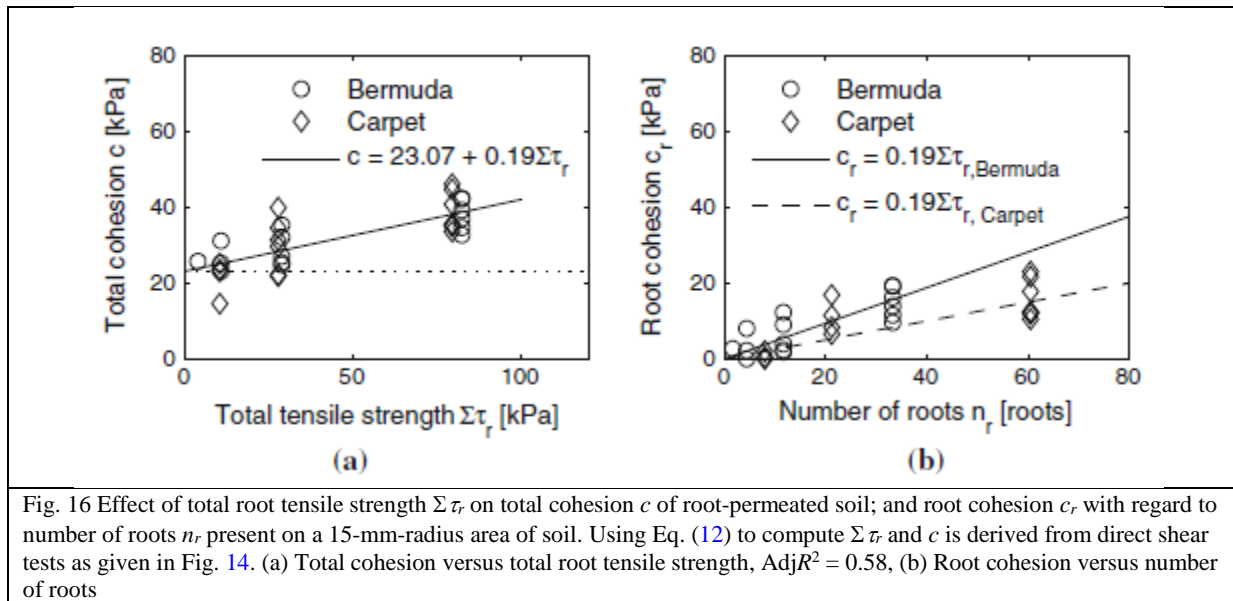
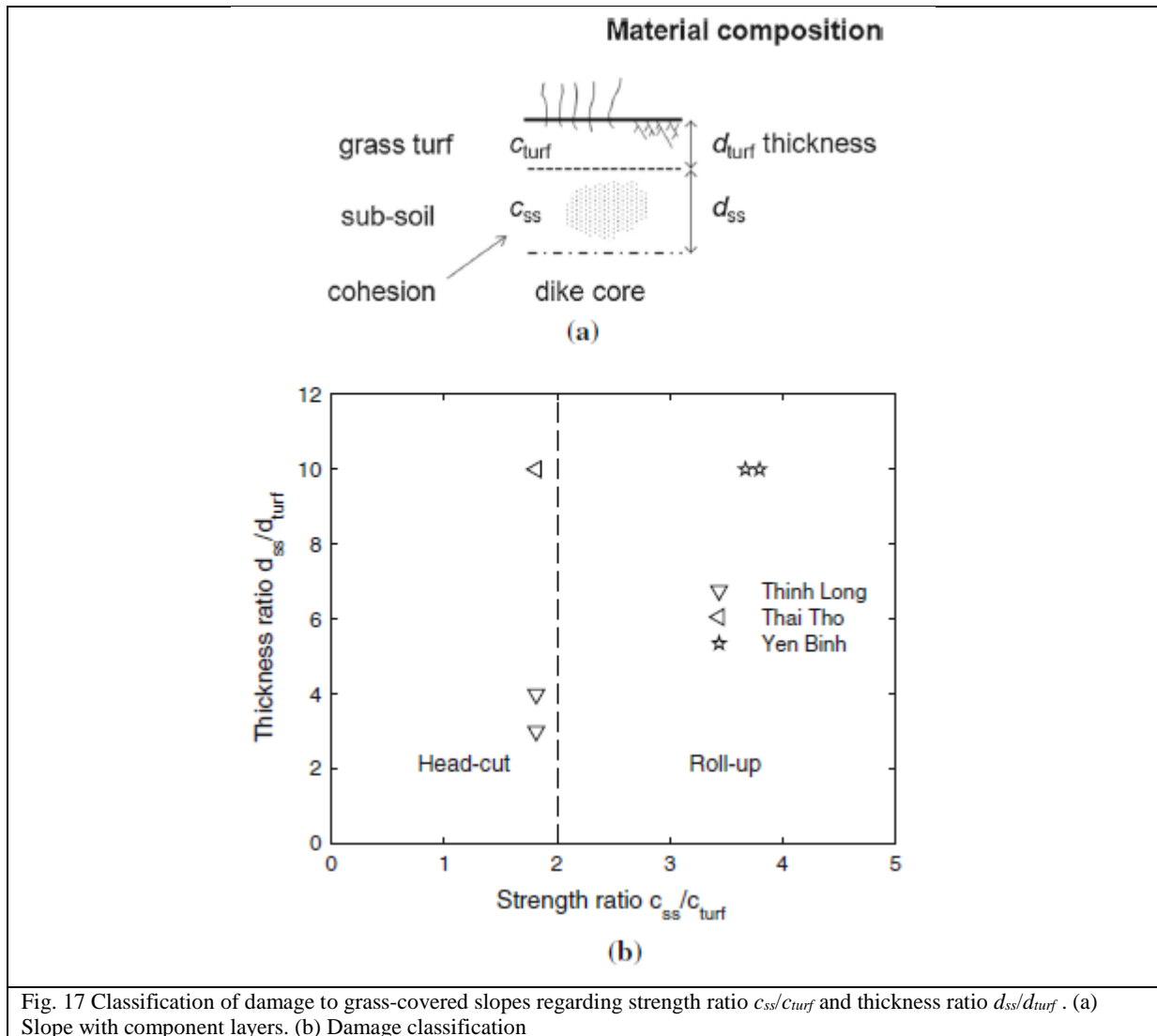


Fig. 16 Effect of total root tensile strength $\Sigma\tau_r$ on total cohesion c of root-permeated soil; and root cohesion c_r with regard to number of roots n_r present on a 15-mm-radius area of soil. Using Eq. (12) to compute $\Sigma\tau_r$ and c is derived from direct shear tests as given in Fig. 14. (a) Total cohesion versus total root tensile strength, $AdjR^2 = 0.58$, (b) Root cohesion versus number of roots

Remarkably, how Bermuda and Carpet roots strengthen soil may be comparable to what is induced by the forest roots in the USA. Schmidt et al. (2001) estimated the cohesive reinforcement to soil due to roots at 41 sites in the Oregon Coast Range, along the Pacific Ocean. Median lateral root cohesion ranges from 6.8 to 23.2 kPa in industrial forests to 25.6–94.3 kPa in natural forests, and uniformly <10 kPa in clearcuts. Note that the root effects were determined at the failure plane due to shear stress, i.e. the amount of root (number, area) was unique at a certain depth.

4.4 Strength ratio and thickness ratio

As discussed in Sect. 2, resistance against overtopping flow of the subsoil and the grass turf mainly governs how damage happens to a dike slope. Therefore, we shall formulate two measurable parameters to predict different damage manners. First, if shear strength is assumed to represent resistance against overtopping flow, we may propose a ratio between cohesion of the subsoil c_{ss} and cohesion at the centre of the turf c_{turf} , as in Fig.17a. Second, the thickness ratio between the two layers d_{ss}/d_{turf} seems to exert some influence on how a slope would fail. The two ratios are estimated for 10 simulator tests in Vietnam and tabulated in Table 4.



The total tensile strength induced by roots makes soil cohesion increase. The greater the number of roots presenting within a turf (higher density), the greater does the total cohesion become. Within a grass turf, we simply assume cohesion of no-root soil as same as of the subsoil. Therefore, c_{turf} would be replaced by the root cohesion $c_r = a_4 \Sigma \tau_r$ that is calculated with Eqs. (12) and (15). For the sake of simplification, we assume a thickness of 20 cm for all grass turfs. Thus, the value of n_r is taken on an area with a diameter of 3 cm and at a depth of 10 cm under the soil surface. We only take into account Bermuda roots when assessing slopes which were covered with more than one grass such as Think Long and Thai Tho. The ratio d_{ss}/d_{turf} is given a rough estimate of 10 in case of clayey dikes like Thai Tho and Yen Binh because the subsoil layer is much thicker than the grass turf. Section 3 would provide root tensile strength τ_r for all test sites, while number of roots n_r are only available for Yen Binh slopes. Therefore, n_{r0} are derived from the Dutch safety standard VTV (2006) for Bermuda at Thai Tho and Think Long with an assumption of good grass covers. The number of roots at the depth of 10 cm is estimated using Eq. (9). Values of c_{ss} are derived from the direct shear tests of the corresponding subsoils.

With greater values of c_{ss}/c_{turf} , the grass covers at Yen Binh were ‘rolled up’, while the ‘head-cut’ took place at Think Long and Thai Tho. A limit of $c_{ss}/c_{turf} = 2$ is proposed to distinguish between the two types. In addition, Vechtdijk is a sand dike and its slope failed with the ‘collapse’ manner due to overtopping flow. The sandy core had a zero cohesion, i.e. ($c_{ss} = 0$). Consequently, points illustrating Vechtdijk tests should lie on the vertical axis. Indeed, these two ratios would be determined for many test points in the Netherlands if strength properties of grass roots and soil are available. By doing so, we may verify this new method of classifying potential damage to grass-covered slopes.

In general, the greater the strength ratio, the higher the possibility that the ‘head-cut’ and ‘roll-up’ types may happen. When the strength ratio goes towards zero, a dike slope is likely to ‘collapse’. If more than one types take place, they should follow a sequence from a ‘roll-up’ or/ and a ‘head-cut’ to a ‘collapse’. On the horizontal

axis, the strength ratio decreases from right to left. Meanwhile, the thickness ratio goes downwards becoming smaller. Remarkably, this sequence is irreversible, i.e. the ‘collapse’ of a grass cover might probably lead to a slope failure, and neither a ‘roll-up’ nor a ‘head-cut’ can take place afterwards.

5 Conclusions

A method has been developed for supporting to predict and classify potential manners of damage to grass-covered dike slopes under attack of overtopping flow. The basic contribution of this paper is that it provides a way to account for the influence of grass roots on how dike slopes would be eroded due to overtopping. To this end, we tested the strength of 10 dike slope sections using a device namely the wave overtopping simulator. Besides, we conducted measurements to explore properties of roots and root-permeated soil on slopes covered with Bermuda, Carpet, Ray and Vetiver grass.

About 70–80% of the total number of roots have diameter varying between 0.1 and 0.2 mm. A single root may withstand a force of up to 10 N. Most roots concentrate within the first 20–30 cm under the soil surface. At a certain depth, the volume and weight of roots are proportional to the number of roots regardless of level and size. About 60–90% of the total amount of roots are present in the first 10 cm under the soil surface. To express how roots distribute, the paper proposed the Root Number Ratio RNR which is the ratio of the number of roots at a certain depth to that at a reference depth (1.5 cm in this paper). An exponential function would probably express the decrease in RNR with increasing depth. The presence of roots improves the shear strength of soil by providing an apparent cohesion, which can be of up to 20 kPa with 1-year-old grass of Bermuda and Carpet. This additional cohesion is proportional to the total root tensile strength $\Sigma \tau_r$, as well as the number of roots present at a certain depth.

The shear strength of a subsoil and a grass turf would be considered to probably represent their resistance against overtopping flow. And many simulator tests have revealed that the relationship between these shear strengths predominantly determines how damage happens to a dike slope. The mechanism ‘head-cut’ gets a high opportunity to happen when the grass turf is as similarly resistant against overtopping flow as the underneath clayey layer (substrate), which should be sufficiently thick. A ‘roll-up’ manner is a shallow erosion temporarily limited within the turf because the substrate is much more durable. By contrast, a sandy core is not able to provide a strong support for a thin grass turf, thus resulting in a ‘collapse’, in which soil aggregates are easily extracted from the turf to fall down. In practice, a combination of these manners may take place on one slope, a ‘roll-up’ or/ and a ‘head-cut’ followed by a ‘collapse’. To classify different manners of damage, the paper formulated two qualitative parameters relating the shear strength and thickness of the grass turf and its underneath layer.

To conclude, the paper illuminates how effectively grass roots may improve shear strength of soil, thus possibly leading to influences on the damage manners of a dike slope. To some extent, the obtained findings contribute to the basis for thoughtfully investigating the strength and failure mechanism of grass-covered slopes under frequent and severe overtopping. Notably, the number and tensile strength of roots tend to gradually increase with grass age. Therefore, grass cover should be properly maintained to reinforce and protect dike slopes better and better.

Acknowledgements A large part of the data presented in this study was mainly achieved through the project ‘‘Technical Assistance for Sea Dike Research’’ supported by the Government of the Netherlands and the project ‘‘Super Sea Dike with high safety level and environmental friendly’’ financed by the Vietnam Ministry of Agriculture and Rural Development. Measurements were taken by the staffs of the Faculty of Marine and Coastal Engineering, Water Resources University and the Plant Protection Research Institute in Hanoi, Vietnam.

References

- Bijlard R (2015) Strength of the grass sod on dikes during wave overtopping. Master thesis, TU Delft, Delft University of Technology, Delft, The Netherlands
- Burger A (1984) Strength of the outer slope of a green dike during a super-storm flood (Sterkte van het buitenbehoop van een groene dijk tijdens een superstormvloed). Technical report, Delft Hydraulics, Delft, The Netherlands
- Cazzuffi D, Cardile G, Gioffre` D (2014) Geosynthetic engineering and vegetation growth in soil reinforcement applications. *Transp Infrastruct Geotechnol* 1:262–300
- Cheng H, Yang X, Liu A, Fu H, Wan M (2003) A study on the performance and mechanism of soilreinforcement by herb root system. In: *Proceedings of third international vetiver conference*, Guangzhou, China, pp 384–390
- Comino E, Marengo P, Rolli V (2010) Root reinforcement effect of different grass species: a comparison between experimental and models results. *Soil Tillage Res* 110:60–68
- Coppin N, Barker D, Morgan R, Rickson R (2007) Use of vegetation in civil engineering. In: *CIRIA C708*. CIRIA, London, UK

Damage to grass dikes due to wave overtopping

- Endo T, Tsuruta T (1969) The effect of the tree's roots upon the shear strength of soil. In: 1968 annual report of the Hokkaido Branch, Forest Exp. Sta, pp 157–182
- Fan C-C, Chen Y-W (2010) Effect of root architecture on the shearing resistance of root-permeated soils. *Ecol Eng* 36:813–826. doi:[10.1016/j.ecoleng.2010.03.003](https://doi.org/10.1016/j.ecoleng.2010.03.003)
- Gray D, Megahan W (1981) Forest vegetation removal and slope stability in the Idaho Batholith. USDA Forest Service Research Paper INT
- Gray D, Ohashi H (1983) Mechanics of fiber reinforcement in sand. *J Geotech Eng ASCE* 109:335–353
- Greenway D (1987) Vegetation and slope stability, *Slope stability: geotechnical engineering and geomorphology*. Wiley, New York, pp 187–230
- Hewlett H, Boorman L, Bramley M (1987) Guide to the design of reinforced grass waterways. In: Construction industry research and information association (CIRIA). London, UK
- Hoffmans G (2012) The influence of turbulence on soil erosion. Eburon Academic Publishers, Delft
- Hoffmans G, Akkerman G, Verhij H, van Hoven A, van der Meer J (2008) The erodibility of grassed inner dike slopes against wave overtopping. In: ASCE, proceedings on 31st ICCE, Hamburg, Germany
- Lambe T, Whitman R (1969) Soil mechanics. Wiley, Hoboken
- Loades K, Bengough A, Bransby M, Hallett P (2010) Planting density influence on fibrous root reinforcement of soils. *Ecol Eng* 36:276–284
- Mickovski S, Bransby M, Bengough A, Davies M, Hallett P (2010) Resistance of simple plant root systems to uplift loads. *Can Geotech J* 47:78–95. doi:[10.1139/T09-076](https://doi.org/10.1139/T09-076)
- Muijs J (1999) Grass cover as a dike revetment. In: Translation of TAW-brochure Grasmat las Dijkbekleding, TAW-brochure, Rijkswaterstaat, Delft, The Netherlands
- MWRI (1991) Sea dikes in Vietnam (in Vietnamese). Technical report, Ministry of Water Resources and Irrigations, Ha Noi, Viet Nam
- O'Loughlin C, Ziemer R (1982) The importance of root strength and deterioration rates upon edaphic stability in steepland forest. In: Proceedings of I.U.F.R.O. workshop P.1.07-00 ecology of subalpine ecosystems as a key to management, pp 70–78. Oregon State University, Corvallis, Oregon
- Piontkowitz T (2009) EroGRASS: failure of grass cover layers at seaward and shoreward dike slopes. In: Design, construction and performance. Technical report
- Pollen N (2007) Temporal and spatial variability in root reinforcement of streambanks: accounting for soil shear strength and moisture. *Catena* 69:197–205. doi:[10.1016/j.catena.2006.05.004](https://doi.org/10.1016/j.catena.2006.05.004)
- Pollen N, Simon A (2005) Estimating the mechanical effects of riparian vegetation on stream bank stability using a fiber bundle model. *Water Resour Res*. doi:[10.1029/2004WR003801](https://doi.org/10.1029/2004WR003801)
- Pullen T, Allsop N, Bruce T, Kortenhaus A, Schu'ttrumpf H, van der Meer J (2007) EurOtop—wave overtopping of sea defences and related structures: assessment manual. EA Environment Agency, UK. ENW Expertise Network Waterkeren, NL. KFKI Kuratorium für Forschung im Küsteningenieurwesen, DE
- Reubens B, Poesen J, Danjon F, Geudens G, Muys B (2007) The role of fine and coarse roots in shallow slope stability and soil erosion control with a focus on root system architecture: a review. *Trees* 21:385–402. doi:[10.1007/s00468-007-0132-4](https://doi.org/10.1007/s00468-007-0132-4)
- Schmidt K, Roering J, Stock J, Dietrich W, Montgomery D, Schaub T (2001) The variability of root cohesion as an influence on shallow landslide susceptibility in the Oregon Coast Range. *Can Geotech J* 38:995–1024. doi:[10.1139/t01-031](https://doi.org/10.1139/t01-031)
- Sprangers J (1999) Vegetation dynamics and erosion resistance of sea dyke grassland. Ph.D. thesis, Wageningen Agriculture University, Wageningen, The Netherlands
- Stanczak G, Oumeraci H (2012) Modeling sea dike breaching induced by breaking wave impact-laboratory experiments and computational model. *Coast Eng* 59:28–37
- Stanczak G, Oumeraci H, Kortenhaus A (2007) Laboratory tests on the erosion of clay revetment of sea dike with and without a grass cover induced by breaking wave impact. FLOODsite report T04-07-11
- Steendam G, Van Hoven A, Van der Meer J, Hoffmans G (2014) Wave overtopping simulator tests on transitions and obstacles at grass covered slopes of dikes. *Coast Eng Proc* 1(34):79
- TCVN8217 (2009) Soil classification for hydraulic engineering (in Vietnamese). Vietnam Ministry of Science and Technology
- Thornton C, van der Meer J, Hughes S (2011) Testing levee slope resiliency at the New Colorado State University Wave Overtopping Test Facility. In: ASCE, proceeding on coastal structures 2011, Yokohama, Japan
- Thornton C, Hughes S, Scholl B, Youngblood N (2014) Estimating grass slope resiliency during wave overtopping: results from full-scale overtopping simulator testing. *Coast Eng Proc* 1(34):52
- Tosi M (2007) Root tensile strength relationships and their slope stability implications of three shrub species in the Northern Apennines (Italy). *Geomorphology* 87:268–283. doi:[10.1016/j.geomorph.2006.09.019](https://doi.org/10.1016/j.geomorph.2006.09.019)
- Trung L (2012) Wave Overtopping Simulator tests on a 1/15 slope protected by two local grass species. In: Communications on hydraulic and geotechnical engineering, 2012-02. Delft University of Technology, Delft
- Trung L, van der Meer J, Schiereck G, Vu M, van der Meer G (2010) Wave overtopping simulator tests in Vietnam. In: ASCE, proceedings on 32nd ICCE, Shanghai, China. <https://journals.tdl.org/ICCE/article/view/1176>
- Trung L, Verhagen H, van der Meer J, Cat V (2012) Strength of the landward slopes of sea dikes in Vietnam. In: Proceedings on COPEDEC VIII, Chennai, India
- Trung L, Van der Meer J, Verhagen H (2014) Wave overtopping simulator tests on Vietnamese sea dikes. *Coast Eng J* 56(03):1450017
- Truong P, Van T, Pinnars E (2008) Vetiver system applications: a technical reference manual. The Vetiver Network International

Damage to grass dikes due to wave overtopping

- Tuan T, Oumeraci H (2012) Numerical modelling of wave overtopping-induced erosion of grassed inner sea-dike slopes. *Nat Hazards* 63:417–447
- Valk A (2009) Wave overtopping—impact of water jets on grassed inner slope transitions. Master thesis, Delft University of Technology, Delft, The Netherlands
- Van Beek L, Wint J, Cammeraat L, Edwards J (2007) Observation and simulation of root reinforcement on abandoned Mediterranean slopes. In: *Eco-and ground bio-engineering: the use of vegetation to improve slope stability*, Springer, pp 91–109
- Van den Bos W (2006) Erosiebestendigheid van Grasbekleding Tijdens Golfoverslag (Erosion resistance of grass covers under wave overtopping). Master thesis, Delft University of Technology, Delft, The Netherlands
- Van der Meer J, Snijders W, Regeling E (2006) The wave overtopping simulator. In: *ASCE, proceedings on 30th ICCE*, San Diego, USA
- Van der Meer J, Steendam G, de Raat G, Bernardini P (2008) Further developments on the wave overtopping simulator. In: *ASCE, proceedings on 31st ICCE*, Hamburg, Germany
- Van der Meer J, Schrijver R, Hardeman, B, van Hoven A, Verheij H, Steendam G (2009) Guidance on erosion resistance of inner slopes of dikes from 3 years of testing with the wave overtopping simulator. In: *ASCE, proceedings on ICE 2009*, pp. 4654–4666, Endinburgh, UK
- Van der Meer J, Hardeman B, Steendam G, Schu'ttrumpf, H, Verheij H (2010) Flow depths and velocities at crest and inner slope of a dike, in theory and with the wave overtopping simulator. In: *ASCE, proceedings on 32nd ICCE*, Shanghai, China
- Van der Meer J, Thornton C, Hughes S (2011) Design and operation of the US wave overtopping simulator. In: *JSCE, proceedings on 6th coastal structures*, Yokohama, Japan
- VTV (2006) Voorschrift Toetsen of Veiligheid Primarie Waterkeringen. Ministry of Transport, Public Works and Water Management
- Waldron L (1977) The shear resistance of root-permeated homogeneous and stratified soil. *Soil Sci Soc Am J* 41:843–849
- Waldron L, Dakessian S (1981) Soil reinforcement by roots: calculation of increased soil shear resistance from root properties. *Soil Sci* 132:427
- Whitehead E, Schiele M, Bull W (1976) *A guide to the use of grass in hydraulic engineering practice*. HR Wallingford
- Wu T (2013) Root reinforcement of soil: review of analytical models, test results, and applications to design. *Can Geotech J* 50:259–274. doi:[10.1139/cgj-2012-0160](https://doi.org/10.1139/cgj-2012-0160)
- Wu T, McKinnell WI, Swanston D (1979) Strength of tree roots and landslides on Prince of Wales Island, Alaska. *Can J Geotech Res* 16:19–33
- Young M (2005) Wave overtopping and grass cover layer failure on the inner slope of dikes. Master thesis, UNESCO—IHE Institute for Water Education, Delft, The Netherlands
- Zhang C-B, Chen L-H, Jiang J, Zhou S (2012) Effects of gauge length and strain rate on the tensile strength of tree roots. *Trees* 26:1577–1584
- Zhang C-B, Chen L-H, Jiang J (2014) Why fine tree roots are stronger than thicker roots: the role of cellulose and lignin in relation to slope stability. *Geomorphology* 206:196–202